

Innovative processing of dense LSGM electrolytes for IT-SOFC's

B. Rambabu*, Samrat Ghosh, Weichang Zhao, Hrudananda Jena

Solid State Ionics Laboratory, Department of Physics, Southern University and A&M College, Baton Rouge, LA 70813, USA

Available online 8 June 2006

Abstract

This paper reports for the first time the attempted synthesis of SrO- and MgO-doped LaGaO₃ (La_{1-x}Sr_xGa_{1-y}Mg_yO_{3-0.5(x+y)}, LSGM) perovskite by an aqueous 'regenerative' solution route. This novel technique enabled recycling of the undesired product and subsequently yielded product with much better phase purity and density than that obtained from the solid-state route. La_{0.8}Sr_{0.2}Ga_{0.85}Mg_{0.15}O_{2.825} (LSGM-2015) and LaGaO₃ were prepared using both the regenerative sol-gel (RSG) and conventional solid-state route at 1400 °C. Series of La_{0.8}Sr_{0.2}Ga_{0.83}Mg_{0.17}O_{2.815} (LSGM-2017) pellets were also prepared by the RSG method at different sintering temperature (1200–1500 °C) and time. The effect of conventional and microwave sintering of samples obtained from both solid-state and regenerative route was also investigated. Microwave heating was carried out using SiC as a microwave susceptor. The LSGM pellets prepared by using different synthetic methods were characterized by X-ray diffraction (XRD), scanning electron microscopy (SEM), electrochemical impedance spectroscopy (EIS) and pellet density was determined by pycnometry. The LSGM-2015 prepared by RSG route exhibited conductivity $\sigma_t = 0.066$ and 0.029 S cm⁻¹ at 800 and 700 °C, respectively, and activation energy of the bulk, grain-boundary, and total are $E_b = 0.97$ eV, $E_{gb} = 1.03$ eV and $E_t = 1.01$ eV, respectively. The sintering temperature severely affected the grain size (<0.1–10 μm) and also the grain-boundary resistance (3–175 kΩ). The unique aspect of this RSG technique is that the final product can be recycled which makes the process cost effective and time saving compared to the solid-state ceramic technique and this technique would allow optimization of processing parameters in a cost effective and time saving manner for obtaining well sintered LSGM as an electrolyte for IT-SOFC's.

Published by Elsevier B.V.

Keywords: Strontium- and magnesium-doped lanthanum gallate (LSGM); Intermediate temperature solid oxide fuel cells (IT-SOFC); Regeneration; Sol-gel synthesis; Crystal growth; Impedance spectroscopy

1. Introduction

In the search for new electrolyte materials, the perovskite-based systems (ABO₃) have been considered as alternative options, particularly because ABO₃ can take on a number of different structures, and can be doped with aliovalent cations on both the A and B sites. They can also accommodate very large concentrations of anion vacancies into their structures. Within the past few years, the La_{1-x}Sr_xGa_{1-y}Mg_yO_{3-0.5(x+y)} has been attracting considerable attentions as very promising alternate electrolyte materials for intermediate temperature solid oxide fuel cells (IT-SOFC) [1–4]. It presents stable, high and almost pure oxide-ion conductivity over a broad range of oxygen partial pressure at operating temperatures equal or below 800 °C [5]. To produce submicron LSGM powders for high-quality

membrane fabrication, the combustion technique via aqueous solutions is usually preferred to the conventional solid-state mixed-oxide method. The solution route provides many advantages, for example, molecular homogeneous precursors, reduced sintering temperature for obtaining dense ceramics, and controllability of uniform superfine grain size [6–12].

However, single phase LSGM with high sintered density is not easy to obtain by conventional solid-state technique. One of the requisites for application as SOFC electrolytes is high sinterability. The extent of sintering depends on the mode of synthesis. The solid-state route results in hard agglomerates and coarser grains which inhibit sintering to obtain dense electrolyte materials. The ball milling of hard agglomerates may cause contamination from the milling and grinding medium. Solution technique, provided homogeneity at molecular level is maintained at all levels of processing, will enable synthesis of these oxides at lower temperature and consequent higher densification. Since solution techniques results in soft agglomerates, ball milling if employed will cause no contamination. Water is a benign solvent and preferable for large scale synthesis.

* Corresponding author. Tel.: +1 225 771 2493; fax: +1 225 771 2310.

E-mail addresses: Rambabu@cox.net, rambabu@grant.phys.subr.edu (B. Rambabu).

Therefore, development of aqueous solution techniques which make use of cheaper precursors will be of great advantage. Since gallium precursors are expensive, therefore, for determination of optimum synthetic conditions necessary for obtaining the desired product with improved properties, recycling of LSGM samples will prove to be cost effective.

For any sol–gel synthesis, phase purity and sintered density of a product depends on the nature of the gel under identical charring conditions. To obtain a phase pure material with high sintered density under less extreme conditions, therefore, several synthetic trials need to be performed which would involve optimization of several gelling parameters such as concentration of the precursor solution, concentration of citric acid, citric acid–glycerol ratio and so forth. Usually in other synthetic approaches for LSGM, this optimization process starts right from the initial step which is weighing of lanthanum, strontium, gallium and magnesium precursors. These leads to preparation of several samples. The advantage of our regenerative sol–gel synthesis lies in recycling of the same product until a better product is obtained in terms of phase purity and sintered density. This makes the process time saving compared to the solid-state ceramic technique. In the regenerative solution technique, the first synthetic trial entails both solid-state ceramic and solution route, whereas the subsequent trials are only solution based. Hence the weighing of individual precursors, their milling and calcination are circumvented which saves time because LSGM obtained in the first trial even if it is not the desired phase can be dissolved in a hot acidic solution to yield a clear solution. This now becomes the precursor solution for the subsequent synthetic trial in which the perovskite LSGM will be regenerated. There are reports of solution synthesis of LSGM in which gallium precursors used were either costly gallium metal or hygroscopic $\text{Ga}(\text{NO}_3)_3 \cdot x\text{H}_2\text{O}$ which requires careful estimation prior to every synthetic process. On the other hand, in our regenerative solution technique, the final product is a combined precursor of Ga, La, Sr and Mg for the subsequent synthetic trial. The combined precursor may not be phase pure but the stoichiometric ratio of the constituents is always retained throughout the synthetic trials. Depending on the particulate properties of the regenerated LSGM, this solid-solution–solid transformation process can be repeated until the processing parameters are optimized.

Recently sol–gel synthesis and microwave sintering of $\text{La}_{0.8}\text{Sr}_{0.2}\text{Ga}_{0.83}\text{Mg}_{0.17}\text{O}_{2.825}$ ($x+y>0.35$) has been reported using costly gallium metal as a precursor [13]. Highly sintered mixed phase sample was obtained by microwave processing at 1500°C for 10 min. To the best of our knowledge there are no reports on recycling of old LSGM samples to obtain new samples of same composition but with different properties. In view of increasing importance to produce dense LSGM ceramics on a large scale with better phase purity at lower temperatures for use as electrolytes, an investigation was carried out to study the effect of conventional and microwave assisted sintering of the recycled LSGM samples obtained from RSG route which is a combination of solid-state reaction and Pechini-type method. This paper reports for the first time an attempt by RSG technique to prepare LSGM ceramic of composition $(\text{La}_{1-x}\text{Sr}_x\text{Ga}_{1-y}\text{Mg}_y\text{O}_{3-0.5(x+y)})$, $x=0.2$, $y=0.15$ – 0.17 , LSGM-2015 and 2017) and investiga-

tion of the effect of conventional and microwave assisted sintering using SiC as a microwave susceptor. LSGM pellets made by the two methods were compared based on their X-ray diffraction (XRD), scanning electron micrography (SEM) and electrochemical impedance spectroscopy (EIS) measurements. The LSGM obtained by RSG method has shown improved properties than the one made by the solid-state method.

2. Experiment

Stoichiometric amounts of La_2O_3 , SrCO_3 , Ga_2O_3 and MgO were ground and heated at 1200°C for 24 h, then ground and heated at 1400°C for 24 h to form the solid-state LSGM precursor. A portion of the solid-state precursor was dissolved in hot doubly distilled water whose pH was adjusted in the range of 0.5–1.0. To 50 ml of the solution, 10 g of citric acid and 5 ml of glycerol were added and dissolved. The resulting solution was introduced into a domestic microwave oven (2.45 GHz; 700 W) and concentrated at maximum power for 10 min to yield a dark brown crisp resin. The resin was calcinated in a muffle furnace at 900°C for 6 h to form the regenerative sol–gel precursor, a kind of soft white powder. The solid-state and RSG precursors were pressed under 230 MPa at room temperature into pellets about 1.4 cm thick and 11 cm in diameter. The pellets were sintered in another furnace (Carbolite RHF 1600) at temperature range of 1200 – 1500°C . A flow chart for the regenerative sol–gel process is shown in Fig. 1.

The sol–gel precursor was ground, milled with PVA as a binder and uniaxially pressed into 11 mm dia pellets under a load of 3 t. For microwave sintering, one of the pellets was kept inside an alumina thermal insulator box (inner dimensions $12\text{ cm} \times 7\text{ cm} \times 10\text{ cm}$) containing SiC as microwave susceptors. This alumina box was then placed in a microwave oven (Panasonic, 2.45 GHz, 1200 W) equipped with a platinum sheathed thermocouple and interfaced with a programmable temperature controller (ThermWave Mod. III, Research Microwave Systems, LLC). The tip of the thermocouple was positioned an inch above the sample pellet mounted between SiC susceptors. Tap water was circulated to prevent overheating of the microwave. On exposure to microwaves at 100% power, the temperature inside the alumina box rose rapidly and reached 1200°C in 30 min and was maintained at that temperature for another 30 min. After heating was over, the alumina box was carefully removed from the oven and allowed to cool in air. To study the effect of different sintering process on phase purity and density, another pellet from the same sol–gel precursor was conventionally heated in air. The temperature of the furnace (Carbolite RHF 1600) was raised at 5°C min^{-1} from room temperature to 1400°C where it was held for 8 h and allowed to cool down to room temperature at 5°C min^{-1} . In order to compare the phase purity and density of the sintered samples obtained from various precursors, a pellet from the ceramic precursor was also conventionally heated in air under the same conditions as above.

The LSGM samples were characterized by XRD, SEM and EIS. The XRD data were taken at room temperature by a

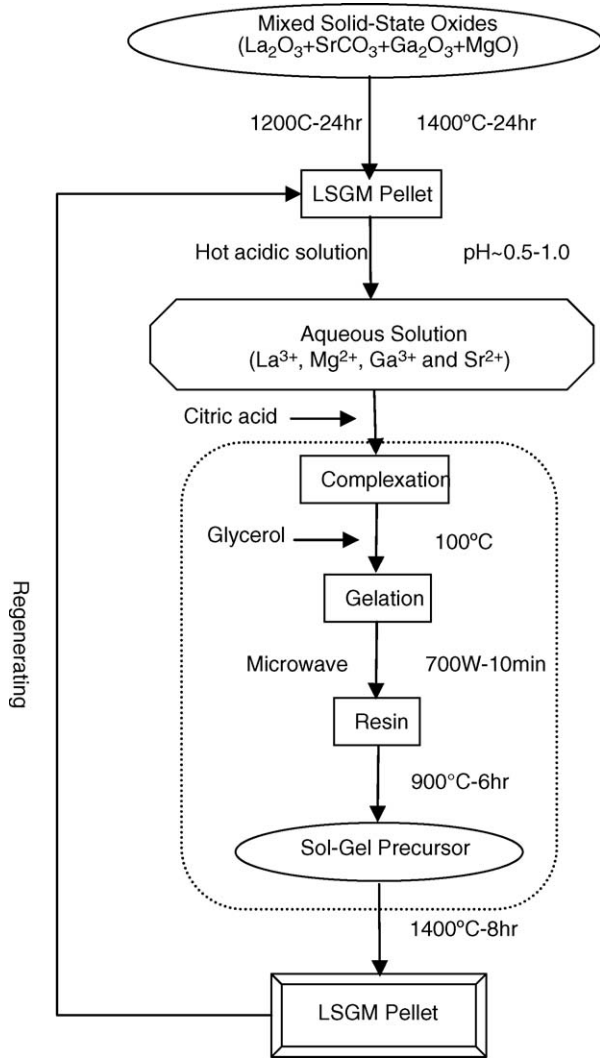


Fig. 1. Flow chart for the regenerative sol-gel process.

Siemens/Bruker D5000 diffractometer using $\text{Cu K}\alpha$ as the incident X-ray. The SEM data were obtained by a JEOL 6300F microscope using 3–5 kV as the accelerating voltages of the electron beam. The EIS measurement (HP-4192A, 5 Hz–13 MHz) of the LSGM-2015 of both solid-state and RSG methods was taken in air at temperature range of 250–850 °C. The two electrodes were made by applying platinum paste to the two sides of the pellet and firing at 980 °C for 30 min. The EIS measurement of the LSGM-2017 prepared in different sintering condition was taken in air at temperature range of 250–500 °C by using Ag-paste made electrodes.

3. Results and discussion

3.1. Comparison of LSGM synthesized by regenerative sol-gel route and solid-state route

LSGM oxides are traditionally recycled through the solid-state method by grinding, pressing and re-sintering. In our experiment, we found the LSGM solid can be dissolved in aqueous solution, and LSGM pellet can be synthesized through

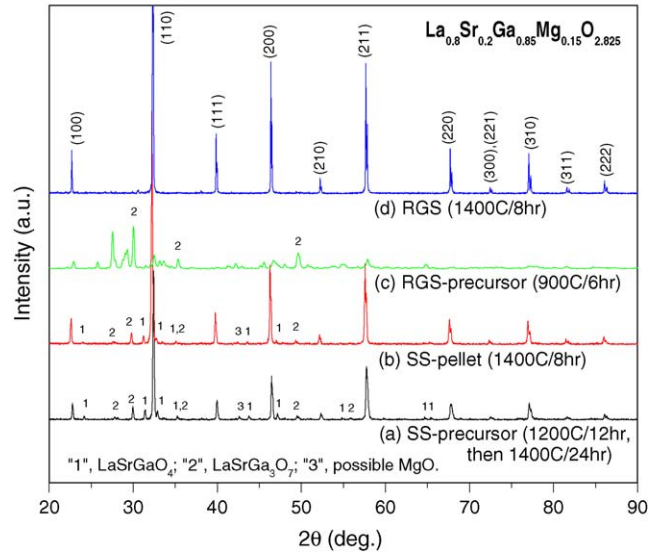


Fig. 2. XRD spectra of $\text{La}_{0.8}\text{Sr}_{0.2}\text{Ga}_{0.85}\text{Mg}_{0.15}\text{O}_{2.825}$ (LSGM-2015): (a) solid-state route precursor; (b) solid-state route pellet starting from the ground powders of (a); (c) regenerative sol-gel route precursor; (d) regenerative sol-gel pellet.

the sol-gel route from the solution. In this way, LSGM can be regenerated also through a solution route, which in general leads to LSGM oxide of superior quality than the solid-state route. To evaluate the physico-chemical properties of LSGM by RSG method, we reproduced LSGM-2015 and LaGaO_3 pellets through both the sol-gel route and the solid-state route starting from the same LSGM-2015 (or LaGaO_3) solid and sintered under the same conditions.

The XRD data in Fig. 2(a) shows the LSGM-2015 precursor obtained by the solid-state reaction (1200 °C for 24 h and 1400 °C for 24 h) has three impurity phases, mainly LaSrGaO_4 and $\text{LaSrGa}_3\text{O}_7$. The peak at $2\theta = 42.2^\circ$ might be from the residue of MgO which is one of the starting oxide material and has very high melting point (2852 °C). The XRD in Fig. 2(b) indicates the recycled LSGM-2015 by solid-state reaction show similar amounts of secondary phases LaSrGaO_4 , $\text{LaSrGa}_3\text{O}_7$ and possible MgO. It was noted that the increased number of sintering cycles did not effectively reduce the secondary phases in the solid-state route LSGM-2015 at 1400 °C. Therefore, to achieve single phase LSGM starting from solid-state oxide mixtures, higher temperature of sintering (~1500 °C) is usually needed [3,12]. Fig. 2(d) shows the formation of pure phase LSGM-2015 at a reduced sintering temperature of 1400 °C by the RSG route. The weak peak near 30.5° is doubted to be a real peak because of its very low counts and may not be assigned to possible impurity phases. The LSGM-2015 precursor (RSG) powders heated at 900 °C and used for pellet pressing were examined by XRD as shown in Fig. 2(c). The broadened peaks in Fig. 2(c) indicate the prevalence of many metastable nanocrystalline phases which are the atomic mixture of cations to the thermodynamically stable LSGM phase.

The SEM micrographs in Fig. 3 exhibit the microscopic surface morphologies of the LSGM precursors and pellets. Fig. 3(a) shows the microstructure of LSGM-2015 pellet obtained from

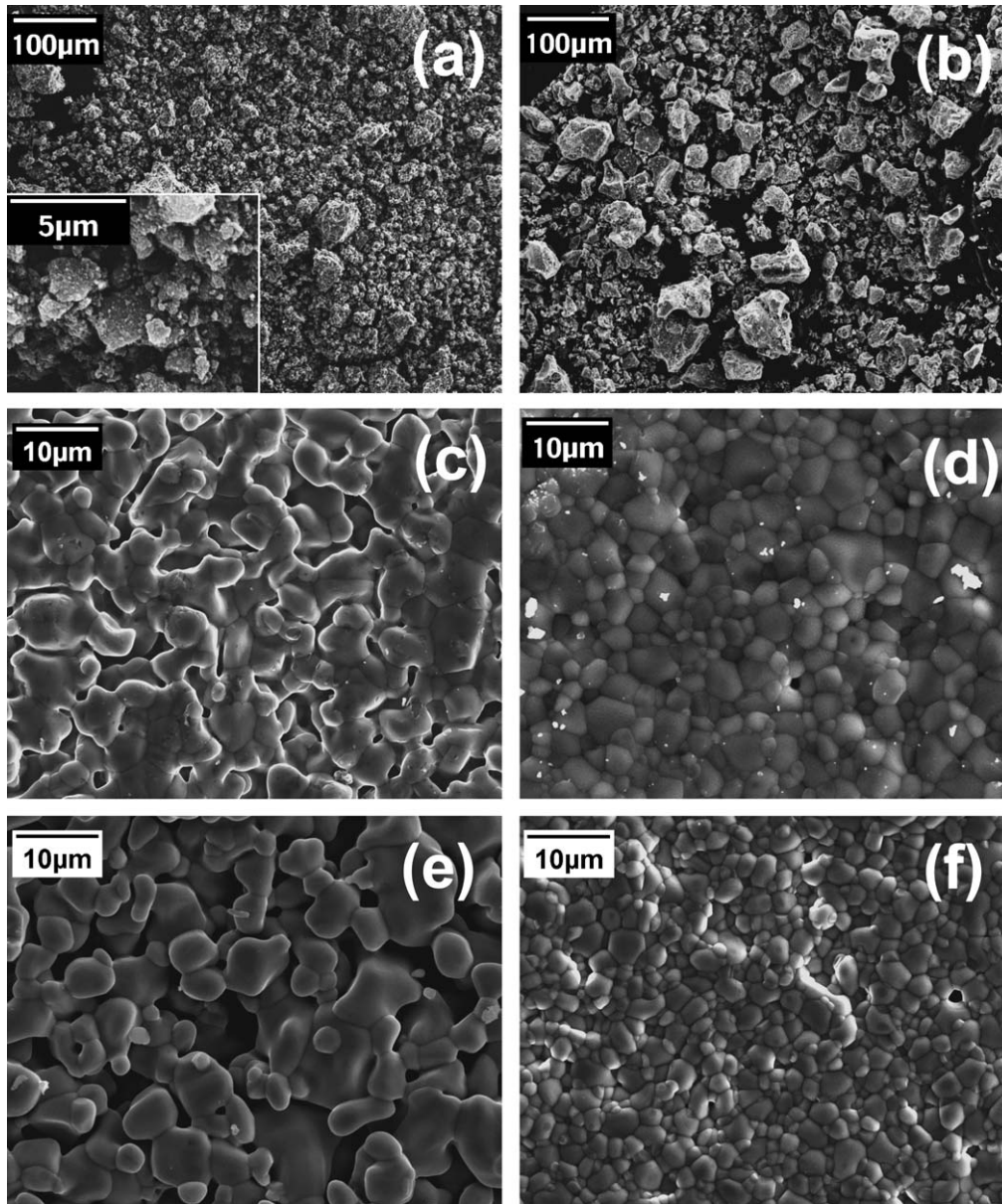


Fig. 3. SEM micrographs of $\text{La}_{0.8}\text{Sr}_{0.2}\text{Ga}_{0.85}\text{Mg}_{0.15}\text{O}_{2.825}$ (LSGM-2015) and LaGaO_3 : (a) solid-state route precursor of LSGM-2015; (b) regenerative sol-gel (RSG) route precursor of LSGM-2015; (c) solid-state route pellet of LSGM-2015; (d) RSG pellet of LSGM-2015; (e) solid-state route pellet of LaGaO_3 ; (f) RSG pellet of LaGaO_3 .

the LSGM-2015 precursor prepared by solid-state reaction route and heated at $1200^\circ\text{C}/24\text{ h}$. The picture in Fig. 3(b) shows the regenerative sol-gel LSGM-2015 precursor heated at 900°C . Although the two precursors show similar microscopic morphologies in the SEM micrograph, their internal crystallization phases are quite different indicated by the XRD in Fig. 2(a) and (c). Fig. 3(a) show the SEM micrograph of LSGM-2015 pelletized and sintered at 1200°C for 24 h (density = 4.29 g cm^{-3} , colour = white). The grain size observed in this micrograph is $\sim 100\text{ }\mu\text{m}$ with large number of voids with no uniform distributions of grains. The pellet re-sintered at $1400^\circ\text{C}/32\text{ h}$ shows coalescing of grains and closing of voids and intergranular spaces leading to pore-free microstructure with a grain size distribution of $5\text{--}10\text{ }\mu\text{m}$ (Fig. 3(c)). The compact microstructure

is further verified from the density measurement (5.25 g cm^{-3} , creamish colour). On the contrary, the SEM micrograph of the pellet obtained from the regenerative sol-gel precursor shown in Fig. 3(d) has highly compact microstructure (5.85 g cm^{-3} , creamish) compared to Fig. 3(b) and (c). The grains are in close contact to each other with distinct grain-boundaries. Ninety percent of the grains are in the range of $1\text{--}5\text{ }\mu\text{m}$. It is noticeable for the similarities in microstructures and grain sizes between the LSGM-2015 and the undoped LaGaO_3 shown in Fig. 3(c) and (e) and in Fig. 3(d) and (f), respectively. Like the LSGM-2015, the reproduced LaGaO_3 through the solid-state route also has plenty of cavities occupying high percentage of the material volume (Fig. 3(e)), but the reproduced LaGaO_3 through the RSG route has compact microstructure (6.46 g cm^{-3} , brown) (Fig. 3(f)).

The similar grain sizes for the LSGM-2015 and LaGaO₃ shown in Fig. 3(c) and (e), respectively, as well as in Fig. 3(d) and (f), indicate the two materials have similar diffusion coefficients even though they have different compositions. The XRD and SEM results in Figs. 2 and 3 have shown the sintering temperature of 1400 °C is high enough for the RSG route to obtain satisfactory dense and single phase LSGM-2015, but not for the solid-state route.

Fig. 4 illustrates the impedance spectroscopy measurement of the LSGM-2015 pellets synthesized by using both the regenerative sol–gel route and solid-state route. The resistances in all bulk and in all grain-boundary (R_b and R_{gb}) of the pellets were estimated from the real axis intercepts of the depressed semicircles based upon the equivalent series circuit of two $R-C$ parallel circuits. The first depressed semicircle near the origin corresponds to the bulk resistance and the second corresponds to the grain-boundary resistance. The first real axis intercept offers the R_b and the second offers the sum of R_b and R_{gb} . The resistances were unified by multiplying the ratio of area to thickness of the measured pellets. Although we got the resistances, because volume fractions of the bulk and grain-boundary are unknown,

it involves complex techniques to calculate the bulk and grain-boundary conductivities. The Arrhenius relations of the bulk and the grain-boundary resistances in Fig. 4(a) indicate the grain-boundary resistance is almost equal to the bulk resistance. Based on the Arrhenius relation of $T/R \propto \exp(-E/k_B T)$, we estimated the activation energies for the oxide-ion conduction across the whole pellet ($E_t = 1.01$ eV), the bulk part ($E_b = 0.97$ eV), and the grain-boundary part ($E_{gb} = 1.03$ eV) by fitting the slopes of the curves in Fig. 4(a). The Arrhenius relation of the total conductivities in Fig. 4(b) indicates the regenerative sol–gel LSGM-2015 has a higher temperature-dependent conductivity than that of the solid-state route LSGM-2015. At 800 and 700 °C, the solid-state route LSGM-2015 has a conductivity $\sigma_t \approx 0.056$ and 0.025 S cm⁻¹, respectively, and the RSG-LSGM-2015 has a conductivity $\sigma_t \approx 0.066$ and 0.029 S cm⁻¹, respectively, which is 16–18% more than the solid-state LSGM-2015 conductivity and is comparable to the conductivity of conventional sol–gel route LSGM starting from liquid-mixing of salt solutions (refer to [6], La_{0.9}Sr_{0.1}Ga_{0.8}Mg_{0.2}O_{2.85}, $\sigma_t \approx 0.065$ and 0.034 S cm⁻¹ at 800 and 700 °C, respectively).

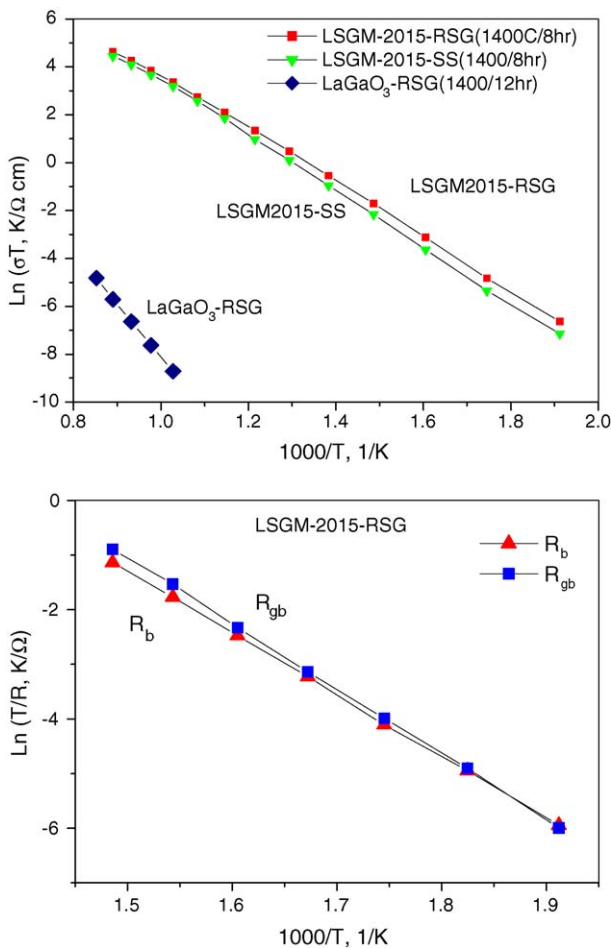


Fig. 4. Impedance spectroscopy of La_{0.8}Sr_{0.2}Ga_{0.85}Mg_{0.15}O_{2.825} (LSGM-2015): (a) Arrhenius relation for conductivities of the solid-state route and regenerative sol–gel route LSGM-2015; (b) Arrhenius relation for bulk and grain-boundary resistances of regenerative sol–gel LSGM-2015.

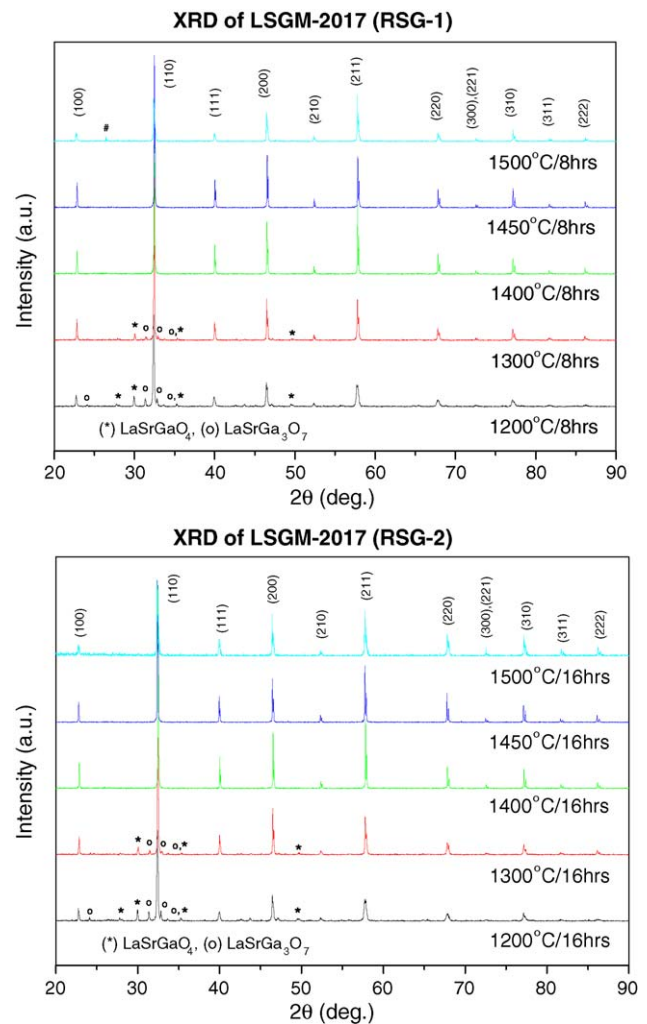


Fig. 5. XRD spectra of regenerative sol–gel route La_{0.8}Sr_{0.2}Ga_{0.83}Mg_{0.17}O_{2.815}: (a) first cycle of sintering for 8 h; (b) second cycle of sintering for 8 h (total 16 h).

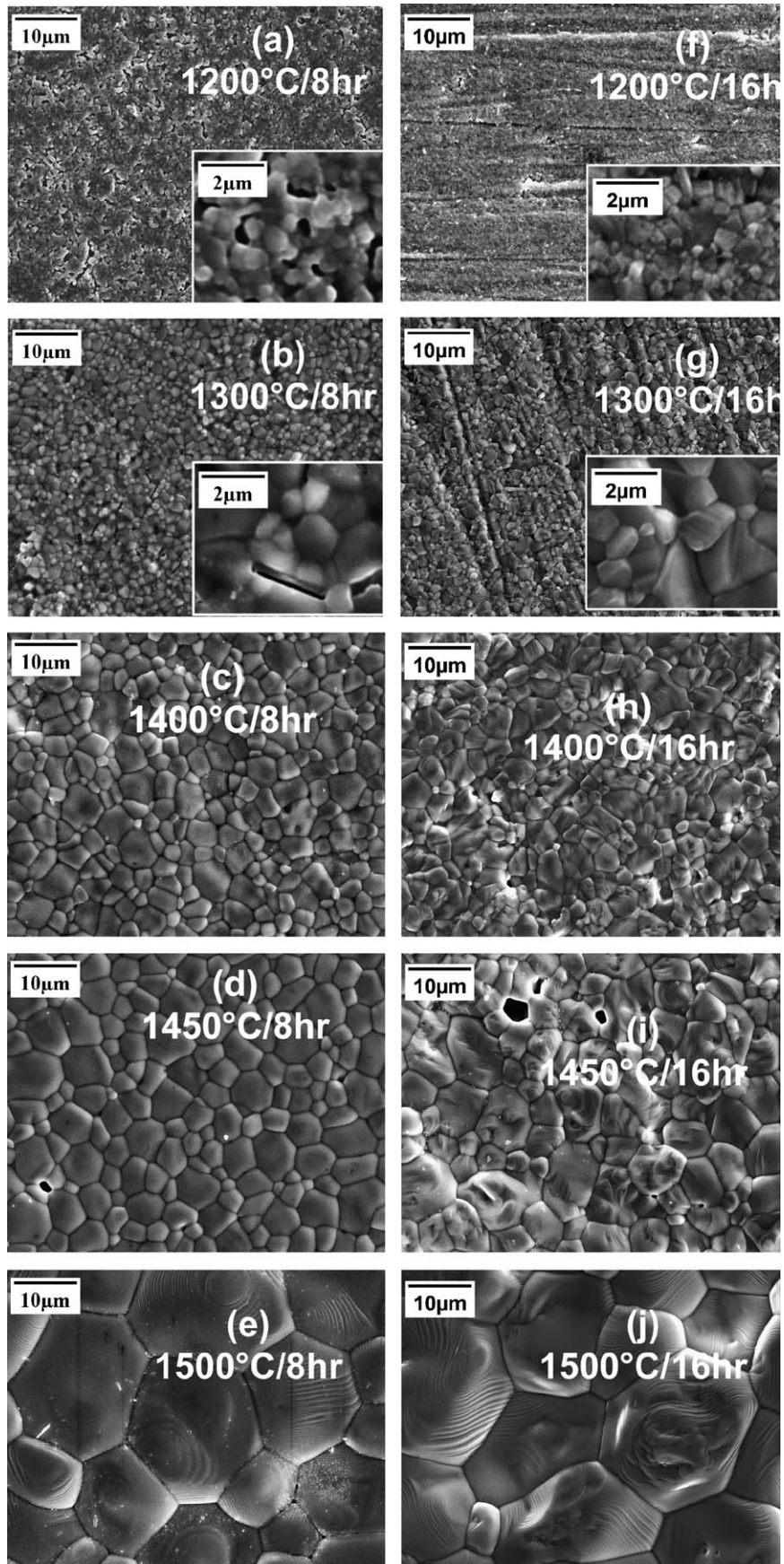


Fig. 6. SEM micrographs of $\text{La}_{0.8}\text{Sr}_{0.2}\text{Ga}_{0.83}\text{Mg}_{0.17}\text{O}_{2.815}$: (a–e) first cycle of sintering for 8 h; (f–j) second cycle of sintering for 8 h (total 16 h).

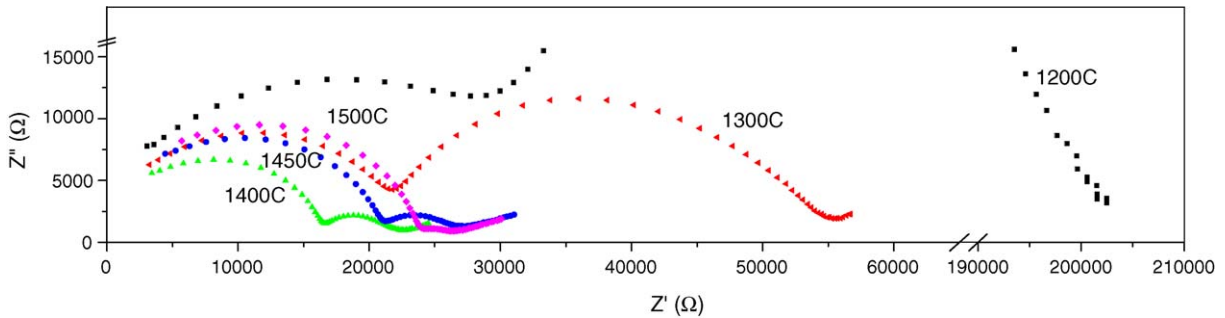


Fig. 7. Complex plane plot of impedance spectroscopy measured in air when the samples are at 325 °C.

3.2. Effects of sintering conditions on LSGM properties

A group of RSG synthesized LSGM-2017 pellets was sintered at five different temperatures, from 1200 to 1500 °C, for 8 h each, and subsequently sintered 8 h. Fig. 5 shows no secondary phase in XRD pattern on the samples sintered at temperature above 1400 °C. The XRD spectra indicate the RSG synthesized LSGM-2017 pellets crystallize in the stable simple-cubic phase at temperature range of 1200–1500 °C. Further, increasing sintering time for 8 h has no effect on the phase formation.

The SEM micrograph in Fig. 6 show the microstructure of LSGM-2017 sintered under different conditions. The grain size is found to be affected severely by the sintering temperature, i.e. higher temperature resulted in bigger average grain size (Fig. 6(a)–(e)). The further sintering helped to diminish those cavities (Fig. 6(a) and (f)), the second cycle of 8 h sintering provided increased grain sizes, (Fig. 6(a)–(e) and (f)–(j)). The grains size of the samples sintered at 1200 °C are very small and most of them are in sub micrometer scale. Whereas the samples prepared by conventional solid-state method did not produce such small LSGM grains with cubic phase. The average grain size of the sample sintered at 1500 °C is ~10 μm. The XRD peaks in Fig. 5 for sample of 1500 °C are not as sharp as those for samples of 1400 and 1450 °C. This observation can be attributed to the melting leading to deformation of the pellet sintered at 1500 °C. There are many interesting wrinkles on the grain surface of the sample of 1500 °C, as shown in Fig. 6(e) and (j). The above phenomena suggest there might be many defects in the grains caused by energetic diffusion at the high temperature of 1500 °C.

Fig. 7 displays the complex-plane impedance spectroscopy measured at 325 °C of the LSGM-2017 samples sintered at different temperatures for 8 h. The samples have similar bulk resistances in the range of 15–30 kΩ, but very diverse grain-boundary resistances from 3 to 175 kΩ. The grain-boundary resistance values are in the inverse order of the sintering temperature. Referring to the SEM pictures in Fig. 6(a)–(e), the sample of 1200 °C has the smallest grains, thus the highest percentage of grain-boundary region, hence the biggest grain-boundary resistance. The sample sintered at 1500 °C has the largest grains, i.e. the smallest grain-boundary region, therefore, smallest grain-boundary resistance in the impedance measurement. Fig. 8 shows the Arrhenius relations for total conductivities, bulk and grain-boundary resistances for the samples sintered at different

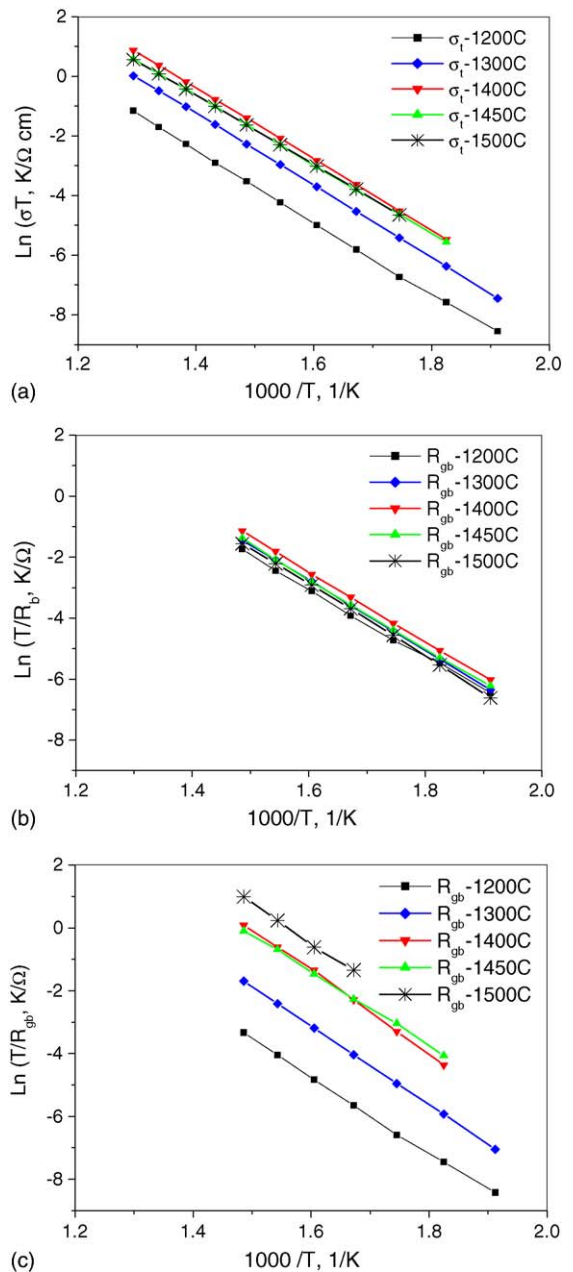


Fig. 8. Arrhenius relation from impedance spectroscopy measurement for regenerative sol–gel route $\text{La}_{0.8}\text{Sr}_{0.2}\text{Ga}_{0.83}\text{Mg}_{0.17}\text{O}_{2.815}$: (a) total conductivity; (b) bulk resistance; (c) grain-boundary resistance.

temperature. There is no significant difference in total conductivities (Fig. 8(a)) of the three samples of 1400, 1450 and 1500 °C. The sample of 1400 °C exhibited the best conductivity. Fig. 8(b) and (c) show the bulk resistances are very close to each other, however, their grain-boundary resistances are quite different. The grain sizes affect severely the grain-boundary resistances compared to the bulk resistance.

4. Conclusion

In summary, the Sr- and Mg-doped and undoped LaGaO₃ oxides can be regenerated through solution route by dissolving the solids in aqueous solution. It is a cost effective way for in-lab or industry synthesis of large amount of LSGM materials which consume expansive gallium containing precursors and also a convenient way to tailor the exact composition by adding solution of certain cation ingredient. The LSGM prepared through the RSG route has higher quality (phase purity, compact microstructure and electrical conductivity) than the solid-state route. The sintering temperature affects the average grain size severely, while the sintering time has little effect on the grain size. The impedance spectra reveal that the smaller the average grain size, the higher grain-boundary resistance; but the bulk resistance almost kept stable and did not change as monotonically along with the grain size as the grain-boundary resistance did.

In conclusion in this paper, we say the merit of regenerative solution technique is the transformation of inhomogeneous system into a homogeneous system. Secondly, the recyclability of the product makes the regenerative solution process cost effective and time saving compared to the solid-state ceramic technique for preparation of phase pure and dense LSGM electrolytes. The process can be repeated till a RSG technique can be extended to other members of the LSGM series. It is well known that performance of SOFC at intermediate temperatures

is enhanced if the electrolytes can be used in the form of thin films. The regenerative solution technique may enable deposition of thin dense films of LSGM on porous anode/cathode substrates by spray pyrolysis, dip or spin coating.

Acknowledgements

The authors acknowledge US-DOE-NETL for providing financial support through grant # DE-FG26-03NT4195. BRB acknowledge US-DOE-NREL for their support to his students in his solid-state ionics (SSI) laboratory. H. Jena thanks the IGCAR (India) for providing the opportunity to work in SSI laboratory at SUBR as an exchange visitor.

References

- [1] T. Ishihara, H. Matsuda, Y. Takita, *J. Am. Chem. Soc.* 116 (1994) 3801–3803.
- [2] M. Feng, J.B. Goodenough, *Eur. J. Solid State Inorg. Chem.* 31 (1994) 663–672.
- [3] K. Huang, R.S. Tichy, J.B. Goodenough, *J. Am. Ceram. Soc.* 81 (10) (1998), 2565–2575, 2576–2580.
- [4] P.-N. Huang, A. Petric, *J. Electrochem. Soc.* 143 (5) (1996) 1644–1648.
- [5] T. Ishihara, M. Honda, T. Shibayama, H. Minami, H. Nishiguchi, Y. Takita, *J. Electrochem. Soc.* 145 (9) (1998) 3177–3183.
- [6] K. Huang, M. Feng, J.B. Goodenough, *J. Am. Ceram. Soc.* 79 (4) (1996) 1100–1104.
- [7] K. Huang, J.B. Goodenough, *J. Solid State Chem.* 136 (1998) 274–283.
- [8] A.C. Tas, P.J. Majewski, F. Aldinger, *J. Am. Ceram. Soc.* 83 (12) (2000) 2954–2960.
- [9] M. Rozumek, P. Majewski, L. Sauter, F. Aldinger, *J. Am. Ceram. Soc.* 86 (11) (2003) 1940–1946.
- [10] H. Jena, B. Rambabu, *Mater. Chem. Phys.* (2006).
- [11] A. Chesnaud, O. Joubert, M.T. Caldes, S. Ghosh, Y. Piffard, L. Brohan, *Chem. Mater.* 16 (2004) 5372–5379.
- [12] J. Wolfenstine, P. Huang, A. Petric, *J. Electrochem. Soc.* 147 (5) (2000) 1668–1670.
- [13] R. Subasri, T. Mathews, O.M. Sreedharan, *Mater. Lett.* 57 (2003) 1792.